RF Performance And Thermal Analysis of AlGaN/GaN Power HEMTs in Presence of Self-Heating Effects

S. Nuttinck[1], E. Gebara[2], J. Laskar[1], B. Wagner[3] and M. Harris[3]

[1] Yamacraw Design Center, School of Electrical and Computer Engineering, Georgia Institute of Technology, Atlanta, GA 30332

[2] Quellan Inc., 250 14th street, Atlanta, GA, 30332

[3] GeorgiaTech Research Institute, Electro-Optics, Environment, and Materials Lab., Atlanta, GA 30332

***Abstract* - Power, linearity and noise performance of AlGaN/GaN power HEMTs are measured at different gate-to-source bias conditions in order to study the influence of self-heating on device RF performance. Additionally, a load-pull system, capable of measuring intermodulation distortion products under pulsed mode of operation, is implemented for the first time. This new system is used to investigate the impact of self-heating on power devices' linearity. Also, for the first time, the effect of the RF drive on thermal effects and power added efficiency (PAE) is investigated. This forms the basis of more accurate nonlinear models. Finally, thermal simulations of 2-finger GaN FETs are performed under pulsed and continuous regime to determine the temperature distribution caused by a 5W/mm power dissipation density.**

I. INTRODUCTION

Power amplifiers, that operate at microwave frequencies, are key elements for applications like phased array radar and base stations. AlGaN/GaN high electron mobility transistors (HEMTs) offer important advantages for high power applications due to the GaN wide bandgap [1-5]. GaN-based FETs offer power densities in the few W/mm range, cutoff frequencies (f_T) above 20GHz, and maximum frequency of oscillation (f_{MAX}) beyond 25 GHz. High power microwave circuits have already been proposed showing the great potential of this technology [6-8].

However, the overall power present in GaN-based power FETs is large and cannot be completely dissipated throughout the substrate. As a consequence AlGaN/GaN HEMTs suffer from self-heating effects. These effects perturb measurement results and reduce the lifetime of the devices under continuous mode of operation. The study of issues, like the reliability of GaN-based devices [9-10], and the understanding of heat dissipation in those transistors [11-12], is still in its early stages, and is crucial to providing a stable technology.

Operating devices during a short period of time permits one to control the heat dissipation in a device. Based on this assessment, pulsed-IV, pulsed S-parameter, and pulsed load-pull systems [11,12,13,14] have been implemented in order to measure heat-free characteristics of high power devices, and to get an in depth understanding of heat dissipation mechanisms, allowing one to build models that integrates thermal effects.

We investigate in Section II the changes of device characteristics under continuous mode of operation when switching from an isothermal environment to a heat regime in order to get a better understanding of self-heating effects on the device microwave performance. In Section III, an innovative load-pull system capable of measuring intermodulation distortion product under pulse mode of operation, is used to study the influence of self-heating on the device linearity. Section IV presents a method to relate thermal effects and PAE. Finally, Section V shows results of thermal simulation of GaN FETs on a SiC substrate, under pulsed and continuous stimulus.

II. SELF-HEATING EFFECTS ON DEVICE RF PERFORMANCE

AlGaN/GaN HEMTs, grown on a SiC substrate, having a total gate width (W_G) of 250µm were studied. They exhibit an f_T of 22GHz, a breakdown voltage between 60 and 80V, and a current density of 800mA/mm. A negative slope is present in $I_{DS}(V_{DS})$ curves under high bias conditions typical of self-heating effects.

We present in this section noise, power and linearity performance of those devices under continuous mode of operation at various gate-to-source bias conditions in order to observe the evolution of the device characteristics when switching from an isothermal environment to a self-heating regime. Drain-to-source voltage (V_{DS}) is fixed at 22V while the gate-to-source voltage (V_{GS}) is varied resulting in a DC power (P_{DC}) sweep from 0.5W to 3.5W.

Noise parameters were measured from 2 to 14GHz using an ATN/Agilent noise measurement system. As shown in Fig.1 the minimum noise figure (F_{MIN}) degrades with increasing frequency and P_{DC}.

The extracted equivalent noise resistance (R_N), presented in Fig.2, is more sensitive to P_{DC} than to the frequency of operation. Its value in the self-heating regime is twice its value under isothermal conditions of operation,

0-7803-7239-5/02/$10.00 © 2002 IEEE

making the device more sensitive to source impedance termination.

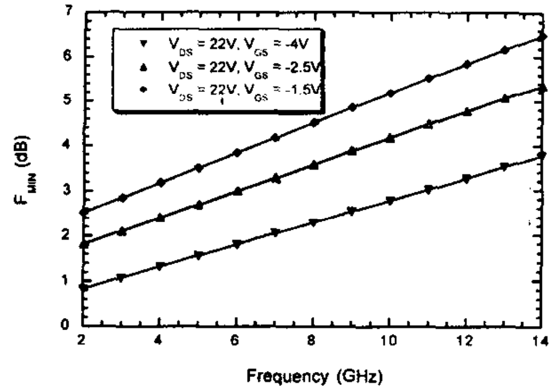

Fig. 1 Extracted minimum noise figure from low to high DC power versus frequency.

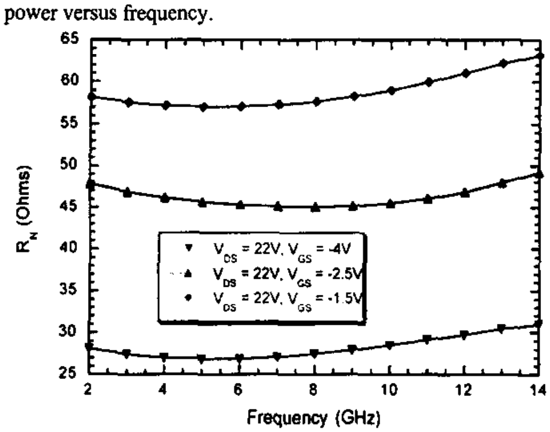

Fig. 2 Extracted equivalent noise resistance from low to high DC power versus frequency.

Power and linearity characteristics are extracted at 8GHz. Load and source impedance are tuned for maximum output power at the 1dB compression point for all bias conditions.

Fig.3 shows power sweep results under high bias condition. A 4W/mm power density is achieved with 27% power added efficiency (PAE), and a gain of 12 dB.

Noise, power and linearity parameters and figures of merit at 8GHz with respect to bias is shown in Table 1. For comparative purposes, the 1dB compression point obtained under each bias condition is chosen for reference.

OP_{1dB} represents output power of the fundamental frequency at the 1dB compression point. IIP3 is the input power of the third order intercept point obtained from intermodulation distortion (IMD) measurements.

In those measurement P_{DC} is increased by reducing the magnitude of V_{GS} while V_{DS} = 22V, resulting in biasing conditions further away from pinch-off. Gain, efficiency and noise performance degrade when increasing P_{DC} while output power and linearity improve.

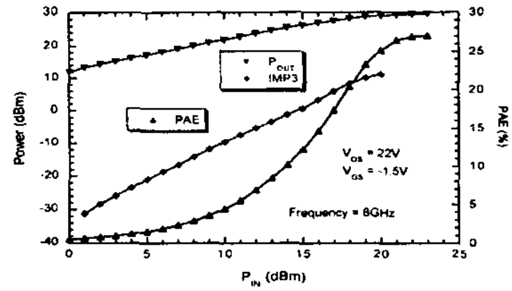

Fig. 3 Power results of an AlGaN/GaN HEMT with W_G=250µm at 8GHz, and at (V_{DS} = 22V; V_{GS} = 1.5V).

	V_{DS} = 22V V_{GS}= -1.5V	V_{DS} = 22V V_{GS}= -2.5V	V_{DS} = 22V V_{GS}= -4V
P_{DC} (W)	3.3	2.2	1
F_{MIN} (dB)	4.5	3.6	2.3
R_N (Ω)	57.6	45	27.9
Gain (dB)	12	13	14.5
OP_{1dB} (dBm)	26.9	25.9	25.5
PAE_{1dB} (%)	14.56	17.18	26
IIP3 (dBm)	24	23	20

Tab. 1 Comparative table of CW performance at 8GHz with respect to the bias condition (dissipated power).

III. Pulsed IMD Measurement System

We present in this section a novel characterization system that allows one to measure intermodulation distortion products under pulse mode of operation. It combines an improved pulsed load-pull system [11-12] and time-gated capabilities of a microwave spectrum analyzer. This system enables one to measure device linearity under high power condition without self-heating effects. Fig.4 shows a schematic of the setup.

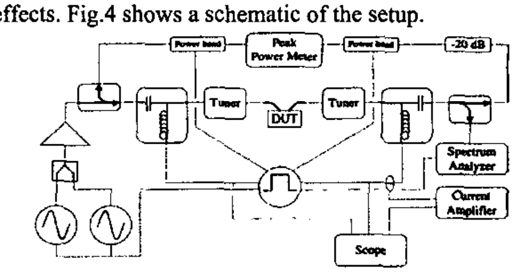

Fig. 4 Schematic of the pulsed load-pull/Intermodulation distortion measurement system.

IMD measurements are performed at 10GHz (V_{DS}=30V and V_{GS}=-0.5V) under continuous mode of operation (I_{DS}#125mA), and under pulsed regime (I_{DS}#144mA) using a pulse width of 5µs and a duty-cycle of 1.6%. Load and source impedance are tuned for maximum output power at the 1dB compression point under each condition of operation.

As shown in Fig.5, an improvement of 2dB of the transistor gain is reported under pulse mode of operation. Consequently, the power of the carrier and the power of the intermodulation distortion products increase. As a result the IIP3 remains about the same, and the OIP3 increases by 2dBm.

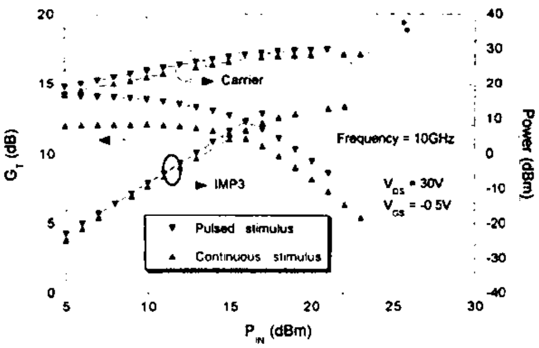

Fig. 5 Pulsed IMD measurement results.

Pulsed IMD measurements are also performed selecting a V_{GS} value that achieves the same drain current as measured under continuous regime. Results are similar and lead to a higher gain and an increase of OIP3 by 2.3dBm.

IV. Self-Heating Effects on PAE

When the total power (P_T) present in a device exceeds its power dissipation capabilities, represented by the power threshold P_{THRES}, the device suffers from thermal effects. The excess of power (ΔP) results in an increase of the device temperature modifying the carrier electronic transport properties and therefore changes the device characteristics [15].

In this section we relate the changes in ΔP caused by an RF drive and the PAE of a device suffering from self-heating effects.

A. Power Threshold

The value of P_{THRES} is determined on a 250µm device using temperature dependent DC-IV measurement results. As reported in [11] the drain voltage threshold where the drain current characteristics degrade increases when decreasing temperature of operation. This allows an accurate determination of the threshold value. Measuring the power threshold at various low temperatures enables accurate extrapolation of P_{THRES} at room temperature.

As shown in Fig.6, a 1.67W P_{THRES} is extracted at 293K.

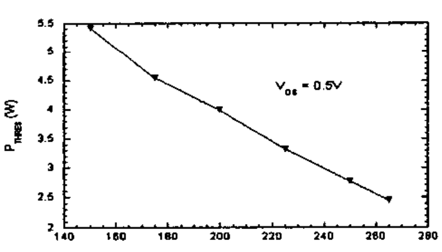

Fig. 6 Extraction of P_{THRES} at 293K.

B. DC Case

The drain current characteristics of a transistor can be expressed at a given bias point with the admittance Y:

$$I_{DS} = Y \cdot V_{DS} \qquad (1)$$

Without an RF drive, the total power present in a device, P_T, can be expressed by:

$$P_T = P_{DC} \approx V_{DS} \cdot I_{DS} \qquad (2)$$

Fig.7 illustrates the variation of the drain current I_{DS} and the variation of the admittance Y with P_T at a given V_{GS}, of a device suffering from self-heating.

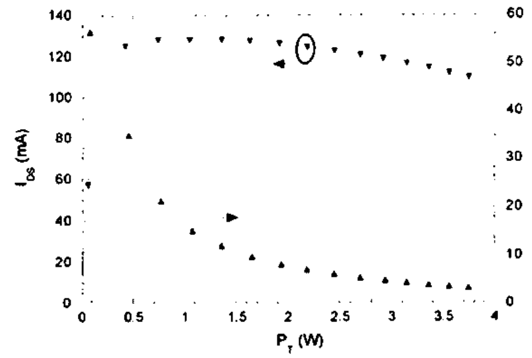

Fig. 7 Admittance Y and drain current I_{DS} versus total power P_T of a 250µm AlGaN/GaN device at fixed V_{GS}.

C. DC + RF Case

In presence of an RF drive P_T can be written as [15]:

$$P_T = P_{DC} + P_{IN}^{RF} - P_{OUT}^{RF} = P_{IN} \cdot (1/PAE - 1) \cdot (G - 1) \qquad (3)$$

where P_{IN} is the power level of the RF drive, and G is the gain. The parameters in Eq.3 can be determined at any bias points and terminations from power measurements. Fig.8 shows a decrease in total power to dissipate in a 250um device when increasing the input power level, and causes a reduction of the thermal effect's magnitude. This results in an increase of the drain-to-source current.

The power added efficiency of a device increases with the input power level. In a class A operation the improvement in PAE starts to become significant when the device goes into compression as P_{DC} decreases while P_{out}-P_{in} increases. In presence of thermal effect, the reduction of P_T causes I_{DS} to increase working against the negative dc component resulting from the harmonics generated by the devices' non-linearity. As a consequence, in presence of thermal effects, the peak PAE is not as high as in a heat free device.

Integration of the thermal effect magnitude changes with the input of the RF drive in nonlinear model would lead to more accurate prediction of the device behavior.

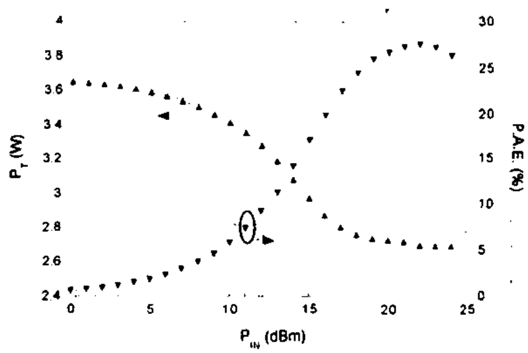

Fig. 8 P_T and PAE versus P_{IN}.

V. Temperature Analysis

A 2 finger GaN FET grown on SiC substrate is modeled as a stack of GaN, (active region = 4μm), SiC (substrate = 13mil), AuSn (solder = 1mil), and CuMoCu (base = 80mil) for thermal analysis purposes. The temperature of the base plate is fixed at 20°C, and simulations are performed under pulsed and continuous condition with a power density to dissipate of 5W/mm.

Fig. 9 shows the peak GaN surface, the GaN/SiC interface and the CuMoCu surface temperatures for a series of 5ms pulses at 25% duty cycle. Timing parameters correspond to those that might be used in pulsed radar applications. A 30°C temperature drop in the thin GaN epi layer is reported, and the peak temperature is about 20°C lower than the continuous wave case (T_{CW} = 96°C).

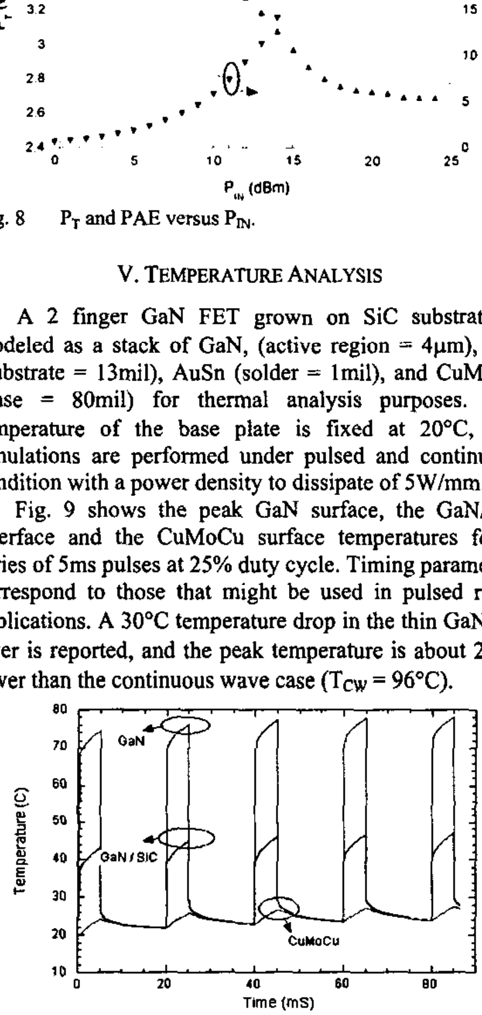

Fig.9 Temperature response at the surface of the GaN layer, at the GaN / SiC interface, and at the CuMoCu surface, under pulsed stimulus.

A temperature of the GaN layer of 300°C has been reported when grown on a sapphire substrate (σ = 0.28W/cm-K) with a base temperature fixed at 30°C [16]. The thermal conductivity of SiC (σ = 3.9W/cm-K) is 14 times higher and results in lower temperature.

VI. Conclusion

Power, noise and linearity measurements have been carried out on-wafer under various power conditions to investigate self-heating effects on AlGaN/GaN power devices. In addition, measurement results using an innovative pulsed IMD system give an in depth understanding of the influence of self-heating on the RF device performance. Also, the influence of thermal effects on the PAE is investigated. Finally, the temperature distribution in GaN FETs under large power density is presented. This study allows one to build more accurate nonlinear models of devices exhibiting thermal effects.

Acknowledgement

The authors wish to acknowledge John Zopler from the Office of Naval Research, CREE Lighting for providing the devices, and Primit Parikh from CREE Lighting for his support.

References

[1] N.Q. Zhang, S. Keller, G. Parish, S. Heikman, S.P. DenBaars, and U.K. Mishra, "High Breakdown GaN HEMT with Overlapping Gate Structure", *IEEE Electron Device Letters*, Vol. 21, No. 9, Sept. 2000.

[2] C.H. Chen, K. Krishnamurthy, S. Keller, G. Parish, M. Rodwell, U.K. Mishra, and Y.F. Wu, " AlGaN/GaN dual-gate modulation-doped field-effect transistors", *Electronics Letters*, Vol. 35, No. 11, May 1999.

[3] S.T. Shepard, K. Doverspike, W.L. Pribble, S.T. Allen, J.W. Palmour, L.T. Kehias, and T.J. Jenkins, "High-Power Microwave GaN/AlGaN HEMT's On Semi-Insulating Silicon Carbide Subtrates", *IEEE Electron Device Letters*, Vol. 20, No 4, pp. 161-163, April 1999.

[4] G.J. Sullivan, M.Y. Chen, J.A. Higgins, J.W. Yang, Q. Chen, R.L. Pierson, and B.T. McDermott, "High-Power 10-GHz Operation Of AlGaN HFET's On Insulating SiC", *IEEE Electron Device Letters*, Vol. 19, No 6, pp. 198-200, June 1998.

[5] U.K. Mishra, Y.F. Wu, B.P. Keller, and S.P. Denbaars, "GaN Microwave Electronics", Topical Symposium on Millimeter Waves. Proceedings, 1997.

[6] Y.F. Wu, R.A. York, S. Keller, B.P. Keller, and U.K. Mishra, "3-9-GHz GaN-based Microwave Power Amplifiers with L-C-R Broad-Band Matching", IEEE Microwave and Guided Wave Letters, Vol. 9, No. 8, Aug. 1999, pp.314 -317.

[7] B.M. Green, K.K. Chu, J.A. Smart, V. Tilak, K. Hyungtak, J.R. Shealy, L.F. Eastman, "Cascode connected AlGaN/GaN HEMTs on SiC substrates", IEEE Microwave and Guided Wave Letters, Vol. 10, No. 8, Aug. 2000, pp.316 -318.

[8] J.J. Xu, Y.F. Wu, S. Keller, G. Parish, S. Heikman, B.J. Thibeault, U.K. Mishra, and R.A. York, "1-8-GHz GaN Based Power Amplifier Using Flip-Chip Bonding", IEEE Microwave and Guided Wave Letters, Vol. 9, No. 7, July. 1999, pp.277 -279.

[9] H. Kim, V. Tilak, B. Green, H. Cha, J.A. smart, J.R. Shealy, and L.F. Eastman, "Degradation Characteristics of AlGaN/GaN High electron Mobility Transistors", IEEE 39th Annual International Reliability Physics Symposium, Orlando, Florida, 2001, pp.214-218.

[10] B.M. Green, K.K. Chu, E.M. Chumbes, J.A. Smart, J.R. Shealy, and L.F. Eastman, "The Effect Of Surface Passivation On The Microwave Characteristics of Undoped AlGaN/GaN HEMT's", IEEE Elect. Dev. Lett., Vol. 21, No. 6, June 2000, pp. 269-270.

[11] S. Nuttinck, E. Gebara, J. Laskar, and M. Harris, "Study Of Self-Heating Effects in GaN HEMTs", IEEE MTT-S 2001, Phoenix, Proceedings, Vol. 3, pp.2151-2123.

[12] S. Nuttinck, E. Gebara, J. Laskar, and M. Harris, "Study Of Self-Heating Effects, Temperature-Dependent Modeling, and Pulsed Load-Pull Measurements on GaN HEMTs", IEEE Trans. On MTT, vol. 49, No.12, December 2001.

[13] M. Liang, and M.E. Law, "Influence Of Latice Self-Heating And Hot-Carrier Transport On Device Performance", *IEEE Trans. Electron Devices*, Vol. 41, No 12, pp. 2391-2398, December 1994.

[14] J. Scott, J. Rathmell, A. Parker, and M. Sayed, "Pulsed device Measurements and applications", IEEE Trans. On M.T.T, vol.44, No.12, Dec.1996.

[15] Y. Zhu, et al., "Analytical Model for Electrical and Thermal Transients of Self-Heating Semiconductor Devices", IEEE. Trans. On M.T.T., Vol.46, No.12, Dec.1998.

[16] Y.F. Wu, B.P. Keller, S. Keller, D. Kapolnek, S.P Denbaars, and U.K. Mishra, "Measured Microwave Power Performance of AlGaN/GaN MODFET", IEEE Electron Device Lett., Vol. 17, No. 9, sept. 1996.